IEEE Access
Multidisciplinary | Rapid Review | Open Access Journal

Received 21 March 2023, accepted 16 April 2023, date of publication 19 April 2023, date of current version 25 April 2023.

Digital Object Identifier 10.1109/ACCESS.2023.3268525

RESEARCH ARTICLE

Estimating Average Power of Welding Process With Emitted Noises Based on Adaptive Neuro Fuzzy Inference System

GOKHAN GOKMEN[1], TAHIR CETIN AKINCI[2,3], (Senior Member, IEEE), GOKHAN KOCYIGIT[4], ISMAIL KIYAK[5], AND M. ILHAN AKBAS[6], (Member, IEEE)

[1]Department of Mechatronics Engineering, Faculty of Technology, Marmara University, 34854 Istanbul, Turkey
[2]WCGEC, University of California at Riverside, Riverside, CA 92521, USA
[3]Department of Electrical Engineering, Istanbul Technical University, 34469 Istanbul, Turkey
[4]Department of Electrical and Electronics Engineering, Trakya University, 22030 Edirne, Turkey
[5]Department of Electrical and Electronics Engineering, Faculty of Technology, Marmara University, 34854 Istanbul, Turkey
[6]Department of Electrical Engineering and Computer Science, Embry-Riddle Aeronautical University, Daytona Beach, FL 32114, USA

Corresponding author: Tahir Cetin Akinci (tahircetin.akinci@ucr.edu)

ABSTRACT In this study, the average power consumption of an electrode welding machine during the welding process was estimated using the features of the sound emitted during welding. First, the instantaneous values of electrode current and voltage and the sound emitted during the welding process were recorded simultaneously. The minimum, maximum, average, root mean square (RMS), and energy values of the sound data were found and feature extraction was performed, and the instantaneous power and average power values were calculated using the instantaneous current and voltage values. Three Adaptive Neuro-Fuzzy Inference Systems (ANFIS) using the sound features as inputs and average power values as outputs were created, and their results were compared. The average power values consumed during the welding process have been successfully estimated at a rate of 87-95%.

INDEX TERMS Welters, average power, emitted noise, neuro-fuzzy inference, data acquisition.

I. INTRODUCTION

Electric arc welding (EAW) is a widely used industrial process that employs an electric arc to fuse the surfaces of metal parts by melting them [1]. The fundamental constituents of an EAW machine comprise a power source, a welding electrode, an arc-forming mechanism, and a welding wire. The power source generates an electric arc between the electrode and the workpiece, the electrode melts and a weld pool is formed, the arc-forming mechanism regulates the distance between the electrode and the workpiece, and the welding wire conducts the current to the workpiece.

EAW machines are widely used in various industrial applications due to their versatility, cost-effectiveness, and ability to join a wide range of metal types and thicknesses [2]. The power source can be direct current (DC) or alternating current (AC), and the electrode can be consumable or non-consumable, depending on the specific application. The arc-forming mechanism is designed to control the arc length and shape, which is crucial for the quality and consistency of the weld. The welding wire is used to transfer the current to the workpiece and can be made of various materials, such as steel, aluminum, or copper.

The use of automation and advanced control systems in EAW machines has led to significant advancements in weld quality and efficiency [3]. The capacity to exert precise control over key parameters, including current, voltage, and travel speed, facilitates enhanced levels of consistency and reproducibility in the welding process. Additionally, the use of real-time monitoring and data analysis has enabled the detection and correction of potential issues during the welding process, leading to further improvements in quality and productivity.

EAW machines are available in a wide range of types and configurations to suit different applications and requirements. The most common types include direct voltage (DC),

The associate editor coordinating the review of this manuscript and approving it for publication was Frederico Guimarães.

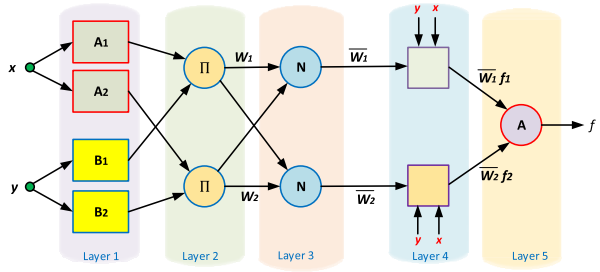

FIGURE 1. A simple ANFIS [33], [34], [35].

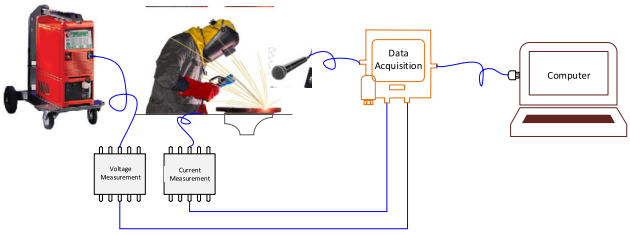

FIGURE 2. The schematic of data acquisition system [38], [39], [40], [41], [42].

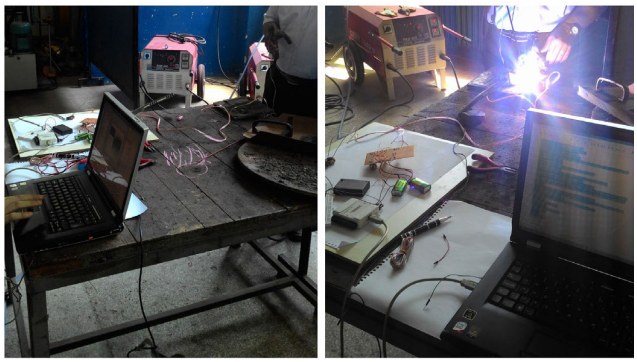

FIGURE 3. A View from welding machine and application.

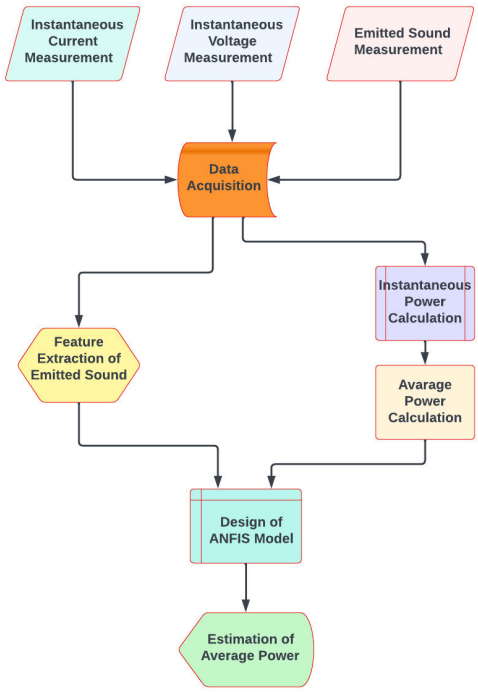

FIGURE 4. Methodology of study.

vertical voltage, and low voltage machines [4]. Direct voltage machines produce a high voltage arc and are typically used for large parts, while vertical voltage machines produce a low voltage arc and are used for smaller parts. Low voltage machines are designed for high precision welding, often used in applications that require high accuracy and minimal distortion.

EAW machines and technologies have undergone significant advancements over the years, particularly in the areas of automation and artificial intelligence (AI) [5]. The integration of advanced control systems and automation has led to improved quality and efficiency in welding processes. Additionally, the use of AI algorithms for real-time monitoring and data analysis has enabled the detection and correction of potential issues during welding, further enhancing the quality and productivity of EAW machines.

The features of EAW machines, such as current, voltage, and frequency, have undergone significant evolution over time. While older machines typically operated with low voltage and high current, modern machines are now able to work with high voltage and low current, resulting in more precise and higher quality welds [6]. Moreover, the frequency response of EAW machines has witnessed a remarkable advancement, with the advent of machines designed to function at diverse frequency amplitudes catering to the distinct application requirements.

In the literature, there are several methods used to analyze the sounds emitted from the electrodes of EAW machines to determine the quality of the welding process and the welding condition of the parts. These methods include frequency, amplitude, and spectrum analysis of the sounds emitted from the welding electrodes [7], [8], [9], [10]. Frequency analysis is used to determine the speed and regularity of the welding process by measuring the number of periodically repetitive segments of sounds emitted from the welding electrodes. Amplitude analysis measures the strength of the sounds emitted from the welding electrodes and is used to determine the intensity of the welding process and the welding condition of the parts [11]. Spectrum analysis examines the frequency composition of the sounds emitted from the welding electrodes and is used to determine the quality of the welding process. A regular welding process will show a uniform distribution, while a distorted welding process will show an uneven distribution. The analysis of the sounds emitted from the welding electrodes is an important tool to monitor and improve the quality and efficiency of welding processes [12], [13], [14], [15].

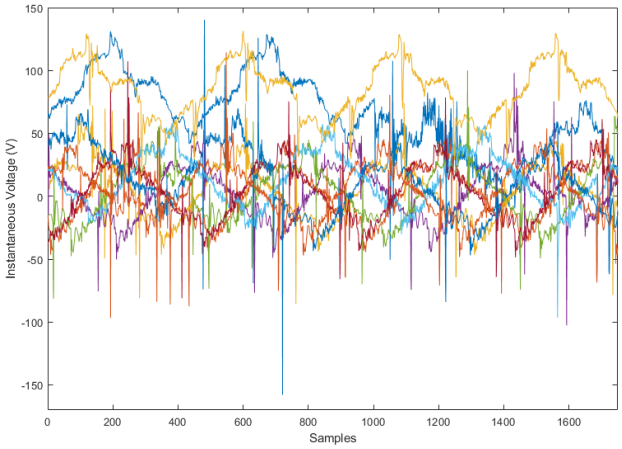

FIGURE 5. Instantaneous electrode voltages (selected 10 values).

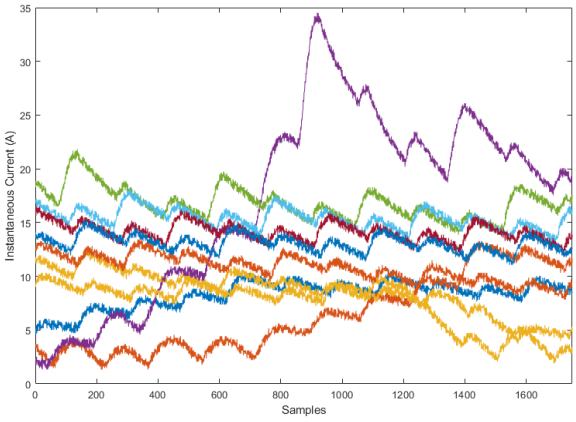

FIGURE 6. Instantaneous electrode currents (selected 10 values).

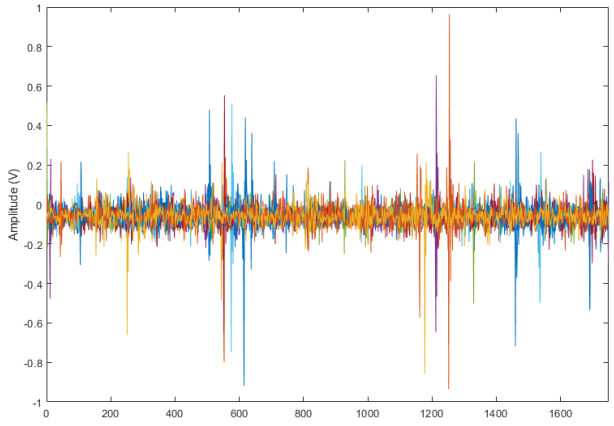

FIGURE 7. Emitted sound pressure (selected 10 values).

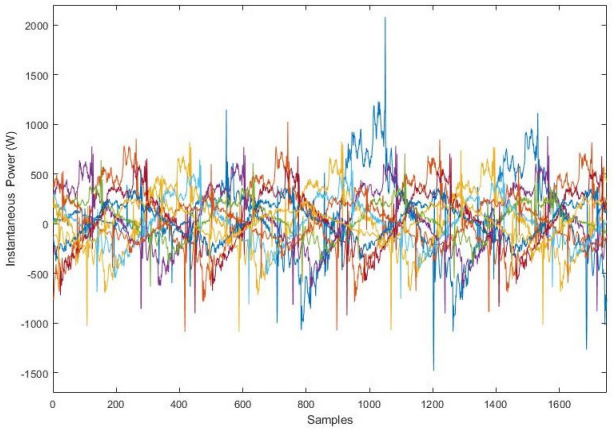

FIGURE 8. Instantaneous electrode power (selected 10 values).

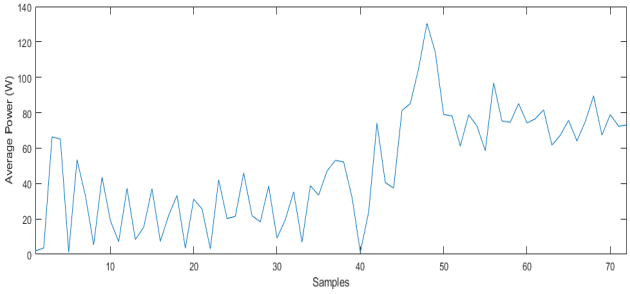

FIGURE 9. Average powers.

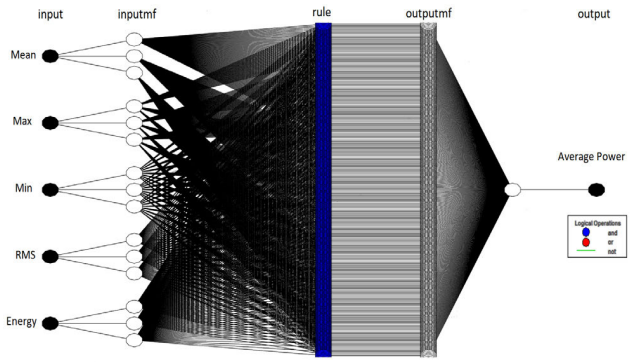

FIGURE 10. The structure of ANFIS model.

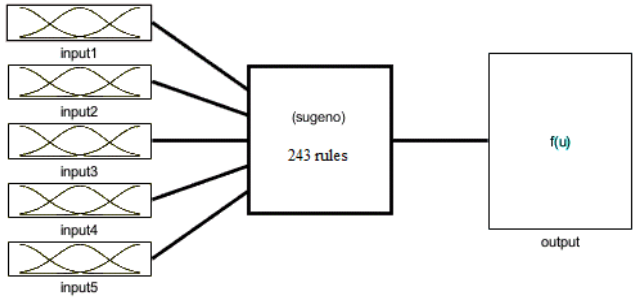

FIGURE 11. Generated FIS models.

In recent years, there has been a growing interest in utilizing Artificial Intelligence (AI) methods to evaluate the effectiveness of EAW machines [16], [17], [18], [19], [20], [21], [22], [23], [24]. These methods are able to provide energy savings and increase the quality of the weld. For example, an Adaptive Neuro Fuzzy Inference System based approach, such as Estimating the Average Power of the Welding Process by Emitted Noise Based Approach, can be used to estimate

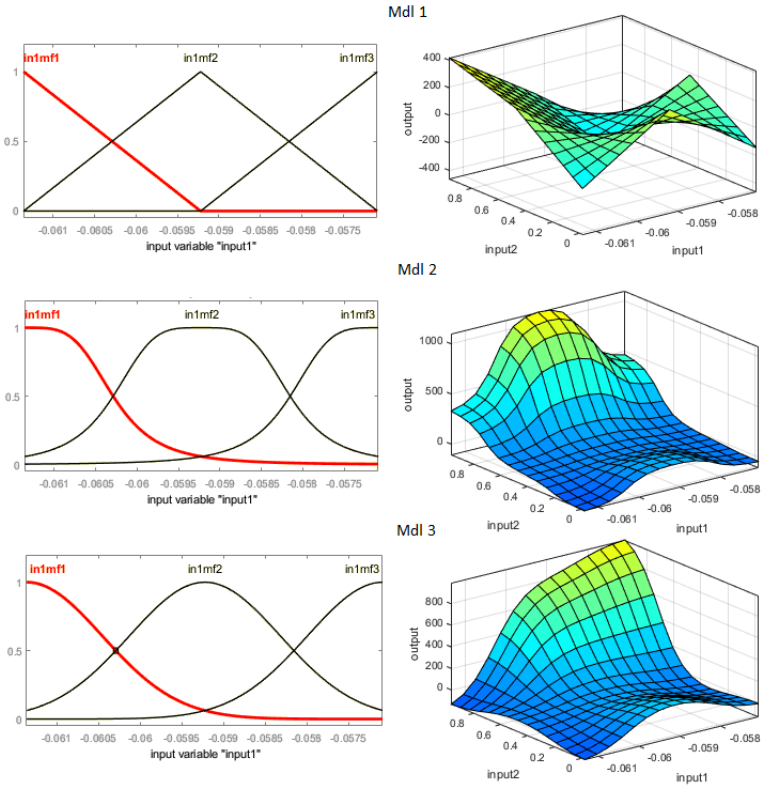

FIGURE 12. FIS membership functions and surfaces of the proposed model.

the average power of the welding process from the noise during welding.

II. WELDING AND SOFT ANALYSIS METHODS

Non-destructive testing (NDT) methods such as X-ray, ultrasonic, and magnetic particle inspection are used in welding industrial analysis to assess the quality of the weld without causing any damage to the joint. These methods are particularly useful in detecting internal defects and imperfections in the weld that may not be visible to the naked eye. Fracture analysis is another important method used in welding industrial analysis. This method involves the examination of a failed weld to determine the cause of the failure and to develop strategies for preventing similar failures in the future.

Simulation and modeling are increasingly being used in welding industrial analysis to predict the behavior of the welded joint under different conditions. These methods use computer simulations to model the welding process and to predict the properties of the welded joint.

The ANFIS method uses fuzzy logic and neural networks to model the relationship between input and output variables, making it a powerful tool for optimizing welding processes and improving the quality of the welded joint.

Welding is a widely-used process in various industries and applications, and there are a variety of methods employed to achieve the desired results. Among the most common methods are:

A. INDUSTRIAL WELDING METHODS

1) METAL INERT GAS (MIG) WELDING

This method involves the use of a welding wire and an inert gas, such as argon or helium, to shield the weld area from the surrounding atmosphere. The wire is fed through a gun and melts as it comes into contact with the workpiece, creating the weld. MIG welding is known for its fast and efficient nature, making it a popular choice for construction and industrial applications.

2) TUNGSTEN INERT GAS (TIG) WELDING

This method involves the use of a tungsten electrode and an inert gas, such as argon or helium, to shield the weld area from the surrounding atmosphere. The electrode is held by the welder and melts as it comes into contact with the workpiece, creating the weld. TIG welding is known for its precision and is often used in industrial applications where high accuracy is required.

3) SHIELDED METAL ARC WELDING (SMAW)

This method involves the use of a consumable electrode and an inert gas, such as argon or helium, to shield the weld area from the surrounding atmosphere. The electrode melts as it comes into contact with the workpiece, creating the weld. SMAW is widely used in remote areas or harsh conditions where other welding methods are not feasible.

Different welding methods are used depending on the application, materials, and conditions. The most common

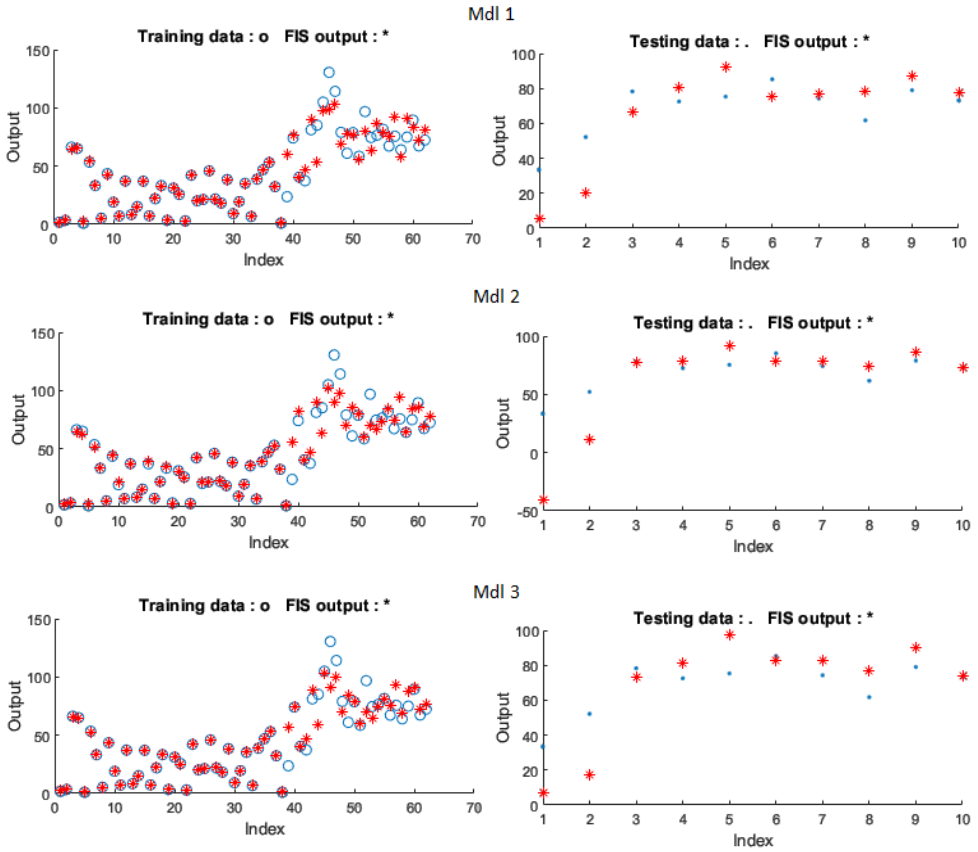

FIGURE 13. Train and test data.

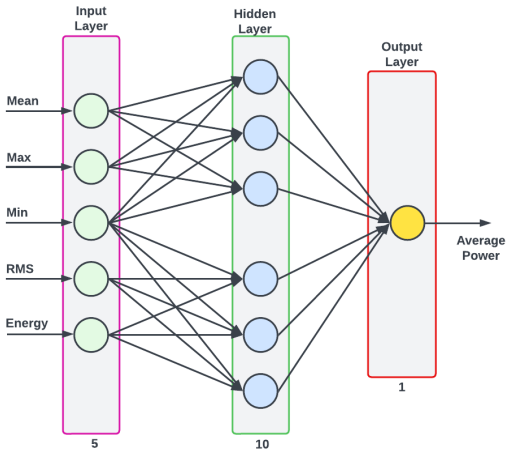

FIGURE 14. ANN model [38].

methods are MIG, TIG and Stick welding methods that used in different conditions and applications.

4) GAS TUNGSTEN ARC WELDING (GTAW)

also known as Tungsten Inert Gas (TIG) welding, is a method that uses a tungsten electrode and an arc-forming gas, such as argon or helium, to create the weld. This method is known for its precision and is frequently used in industrial applications.

5) SUBMERGED ARC WELDING (SAW)

is another method that uses a welding wire, welding electrode, and arc-forming gas, such as argon or helium, to create the weld. This method is typically used for large parts and is often employed in construction and industrial applications.

B. INDUSTRIAL WELDINGS ANALYSIS METHODS

Flux Cored Arc Welding (FCAW): is a method that uses a welding electrode that contains flux. The flux is used to cause arcing and clean the oxides on the surface of the metal during welding [25], [26], [27].

1) ARTIFICIAL INTELLIGENCE (AI)

methods can be used to improve the quality of the weld. These methods include:

2) CLASSIFICATION BASED ON LEARNING

This method is used to classify the quality of the source using audio and video data generated during the welding process. Learning-based classification plays an important role in determining and improving the quality of the welding process.

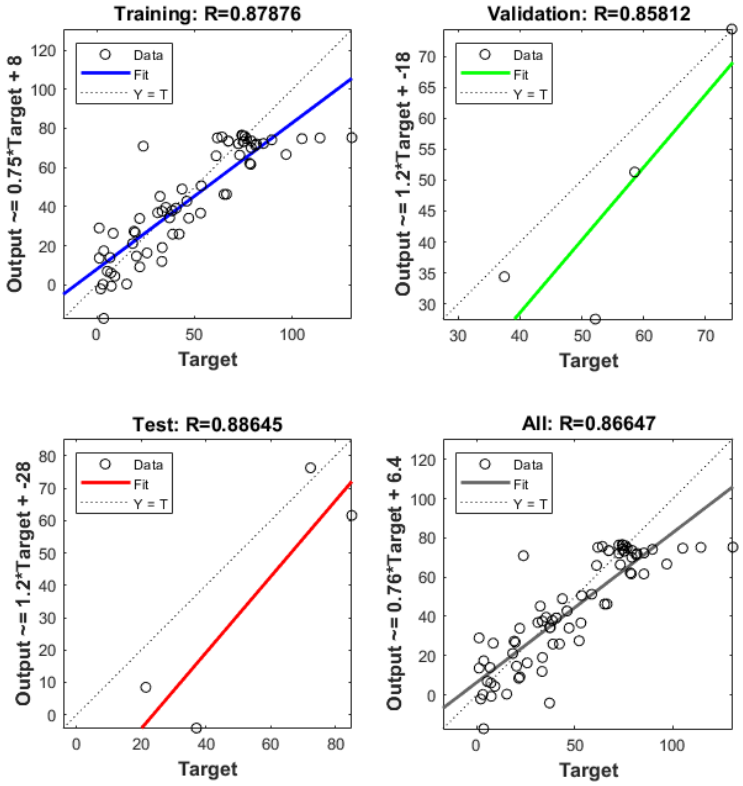

FIGURE 15. ANN regression results.

3) DEEP LEARNING

Deep learning methods are used to predict the quality of the source using audio and video data generated during the welding process. Deep learning plays an important role in determining and improving the quality of the welding process.

4) CONTROL SYSTEMS

AI control systems can be used to control the parameters of the welding process. This method can be used to improve the quality of the welding process.

5) OPTIMIZATION

AI optimization methods can be used to optimize the parameters of the welding process. This method can be used to improve the quality of the welding process.

6) ANOMALY DETECTION

Artificial intelligence anomaly detection methods can detect malfunctions and malfunctions that may occur in the welding process. This method can be used to improve the quality of the welding process [28], [29], [30], [31], [32].

It is important to note that while there are many methods available to improve weld quality using AI, the success of the method varies depending on the material used. Therefore, it is essential to determine the appropriate method according to the characteristics of the project and the material.

III. ADAPTIVE NEURO FUZZY INFERENCE SYSTEM (ANFIS)

ANFIS (Adaptive Neuro-Fuzzy Inference System) is one of the most common hybrid models, which uses both Fuzzy Logic and Artificial Neural Networks (ANN) together. It has the flexibility of Fuzzy Logic, in addition to the classification ability of ANN, making it very popular for solving non-linear problems. Fuzzy Inference System (FIS) and ANFIS are rule-based models, but it is not always easy to determine the rule base [33], [34], [35], [36]. To overcome this problem, Jang proposed optimizing FIS parameters with ANN [4]. The ANN generates Takagi-Sugeno type if-then rules. The if-then rules for a simple Sugeno type fuzzy model are given below, where x and y represent two inputs [33], [34], [35], [36], [37].

$$\begin{aligned} &\text{if } x \text{ is } X_1 \text{ and } y \text{ is } Y_1 \text{ then } f_1 = p_1 x + q_1 y + r_1 \\ &\text{if } x \text{ is } X_2 \text{ and } y \text{ is } Y_2 \text{ then } f_2 = p_2 x + q_2 y + r_2 \end{aligned} \quad (1)$$

In this equation, X_i and Y_i are the input fuzzy sets, f_i is the output, p_i, p_i and r_i are the design parameters determined during the learning phase [33], [34], [35].

An ANFIS model has 5 layers. The initial layer is the defuzzification layer and assigns the membership value for each input. Expression of nodes at the input layer are;

$$o_i^1 = \mu_{X_i}(x), \quad \text{for } i = 1, 2 \quad (2)$$

Defuzzification is determined by the shape of the assigned membership function. It could be Gaussian or bell curve, triangular, trapezoidal [33], [34], [35], [36], [37].

The second layer is where the fuzzy rules are activated and multiply the data from the first layer [33], [34], [35], [36], [37].

$$o_i^2 = w_i = \mu_{X_i}(x) \times \mu_{Y_i}(y), \quad for\ i = 1, 2 \tag{3}$$

The third layer is the normalization of the firing powers of the fuzzy rules [33], [34], [35], [36], [37].

$$o_i^3 = \overline{w}_i = \frac{w_i}{w_1 + w_2}, \quad for\ i = 1, 2 \tag{4}$$

The fourth layer is responsible for defuzzification by multiplying the normalized firing powers by the linear function or constant determined by each rule [33], [34], [35], [36], [37].

$$o_i^4 = \overline{w}_i \times f_i = \overline{w}_i \times (p_i x + q_i y + r_i) \quad for\ i = 1, 2 \tag{5}$$

The fifth layer is the final layer where all outputs are collected [33], [34], [35], [36], [37].

$$o_i^5 = \sum \overline{w}_i \times f_i, \quad for\ i = 1, 2 \tag{6}$$

In ANFIS, adaptation occurs at two layers during the training phase. The first layer is responsible for adjusting the precondition parameters, while the fourth layer is responsible for adjusting the outcome parameters. The Hybrid Learning Algorithm employed in ANFIS consists of two phases: the forward pass and the backward pass. During the forward pass, the precondition parameters are held constant while the outcome parameters are calculated using the least squares method. In the backward pass, the outcome parameters are held constant, and the precondition parameters are calculated by back-propagating the error rates and gradually decreasing them, as outlined in the literature [33], [34], [35], [36].

IV. DATA ACQUISITION SYSTEM

The data acquisition system employed in the study, as shown in Figure 2, comprised of a microphone, current and voltage transducers, and a National Instruments USB-6009 data acquisition card. The instantaneous voltage at the electrode terminals, the instantaneous electrode current, and the sounds emitted during welding was recorded using an electrode welding machine with a sampling frequency of 24 kHz. In order to measure the power of the welding process, direct measurements of the instantaneous current and voltage of the electrode were obtained. Efforts were made to minimize the impact of environmental noise through the use of active noise cancellation techniques. The study was conducted in the welding laboratory of Kirklareli Vocational High School.

V. APPLICATION AND ANALYSIS

The power consumption of the welding machines can be calculated from the line voltage and the current of the electrical network; however, the result also includes machine power losses. The power consumption of the welding process can only be directly calculated by measuring the electrode voltage and current. Detecting the sound emitted during the welding process can provide an indirect calculation of the power consumption. First of all, the average power values should be calculated from the instantaneous voltage and current data obtained by the data acquisition system, and the characteristics of the emitted sound data should be extracted. Thus, an ANFIS model with sound characteristics as inputs and average power as the output can be designed (Fig 4).

Seventy-two sets of instantaneous voltage, instantaneous current, and emitted sound data with 1,750 samples were recorded sequentially by the data acquisition system. (Fig. 5, 6 and 7).

While the electrode's instantaneous voltage at idle is around + 140 V, it changes polarity during welding and takes a value around −150 V. The electrode's instantaneous current is around +35 A and does not change direction. This situation demonstrates the inductive load characteristic of the welding machine. By multiplying the instantaneous voltage and current values, the instantaneous power consumed during welding can be determined (Fig. 8).

The instantaneous power variation varies between approximately +2kW and −1.5 kW, with positive values representing the power dissipated during welding and negative values representing the power returned. However, when we calculate the average power values, the average power change during the welding process gives us a more meaningful parameter (Fig 9) [43].

$$P[n] = \frac{1}{N} \sum_{n=1}^{N} p[n], \quad for\ n = 1, 2 \ldots, N \tag{7}$$

The average of these 72 instantaneous power datasets ranges between approximately 131 and 0 W.

To develop a suitable ANFIS model, feature extraction methods can be applied to the dataset shown in Fig. 7 to obtain input values for average power estimation. The preferred methods are average, maximum, minimum, RMS values and energy value [44].

$$s_{mean} = \frac{1}{N} \sum_{n=1}^{N} s[n], \quad for\ n = 1, 2 \ldots, N \tag{8}$$

$$s_{\max} = \max\{s[n]\}, \quad for\ n = 1, 2 \ldots, N \tag{9}$$

$$s_{\min} = \min\{s[n]\}, \quad for\ n = 1, 2 \ldots, N \tag{10}$$

$$s_{rms} = \sqrt{\frac{1}{N} \sum_{n=1}^{N} (s[n])^2}, \quad for\ n = 1, 2 \ldots, N \tag{11}$$

$$s_{energy} = \sum_{n=1}^{N} (s[n])^2, \quad for\ n = 1, 2 \ldots, N \tag{12}$$

According to the data in Table 1, the proposed ANFIS model has five input variables: the average, maximum, minimum, RMS values of the emitted sound data, and the energy value. The average power values given in Fig. 9 are the output of the model. The structure of ANFIS model is shown Fig 10.

Each input variable has five membership functions and 243 rules are created. Gaussian, bell curve, or triangular

TABLE 1. Feature extractions of emitted sounds.

	Mean	*Max*	*Min*	*RMS*	*Energy*
S_1	-0.057960741	0.036758984	-0.186236362	0.063229095	6.996357285
S_2	-0.060891781	0.256092164	-0.609552148	0.071939585	9.056781914
S_3	-0.058786611	0.104966812	-0.229236286	0.068676649	8.253843761
S_4	-0.059401890	0.220508125	-0.383321889	0.070899798	8.796867413
S_5	-0.059530798	0.105607691	-0.218707561	0.069791495	8.523992292
S_6	-0.058427649	0.229114214	-0.372457465	0.069593912	8.475797138
S_7	-0.059966212	0.212909133	-0.858213169	0.076238310	10.17148986
S_8	-0.057865524	0.145891508	-0.704982071	0.075732863	10.03706637
S_9	-0.059585085	0.232135500	-0.269306477	0.070604391	8.723715143
S_{10}	-0.057960741	0.036758984	-0.186236362	0.063229095	6.996357285
.	.	.	.	.	.
.	.	.	.	.	.
.	.	.	.	.	.
S_{62}	-0.059293281	-0.024765393	-0.089402609	0.060347295	6.373143093
S_{63}	-0.059115421	-0.015243763	-0.095475700	0.060385592	6.381234497
S_{64}	-0.059776669	-0.023208972	-0.094743267	0.060941544	6.499275569
S_{65}	-0.060507829	-0.025711452	-0.096635386	0.061711363	6.664511601
S_{66}	-0.058933080	-0.027969787	-0.096330205	0.060012557	6.302637254
S_{67}	-0.059237494	-0.025223163	-0.091966125	0.060486364	6.402550318
S_{68}	-0.059035272	-0.021683070	-0.090562295	0.060189177	6.339789881
S_{69}	-0.059121787	-0.022781720	-0.096543832	0.060351635	6.374059728
S_{70}	-0.060229487	-0.021469444	-0.093644617	0.061313820	6.578922849
S_{71}	-0.058269845	-0.026047150	-0.097459373	0.059333782	6.160870956
S_{72}	-0.059293281	-0.024765393	-0.089402609	0.060347295	6.373143093

TABLE 2. Training and testing errors of results of ANFIS.

Models	*Input MF*	*Number of MF*	*Output MF*	*RMSE (Training)*	*RMSE (Testing)*	R^2 *(Training)*	R^2 *(Testing)*
Md1 1	triangle	15	constant	9.328812	16.6632889	0.955091392	0.875212
Md1 2	gbell	15	constant	9.666645	27.9565657	0.951779213	0.932452
Mdl 3	gauss	15	constant	9.641569	17.1865578	0.951971778	0.894970

membership functions are used to fuzzify all inputs. For the output, a constant membership function was preferred. The FIS models generated by ANFIS are shown in in Fig 11.

Membership functions and surfaces of FIS models are shown in Fig. 12. The model results are generally compatible with one another, and it was possible to obtain lower RMSEs in Mdl1 and Mdl3.

VI. COMPARISON OF ANN AND ANFIS RESULTS

Artificial neural networks (ANN), which are another common estimation method, were used to compare the performance of the ANFIS models we obtained. For this purpose, a feedforward ANN model was created. As in the ANFIS model, the selected five audio features constituted the inputs, and the average power was the output. Therefore, there were five neurons in the input layer and one neuron in the output layer. There were ten neurons in the hidden layer (Fig. 14).

The Levenberg-Marquardt algorithm was preferred for training. The tangent function was chosen for activation. Sixty-four samples were used for training, four for testing, and four for validation. The root mean squared error was obtained as 15.6911 for training, 12.9097 for validation, and 24.6559 for testing. Regression results are shown in Fig. 15.

In order to compare the performances of ANFIS and ANN models, the outputs of the models and errors are given in Fig. 16-19.

When comparing ANFIS and ANN models, it can be said that the outputs of ANFIS models are more compatible with each other. Error values are generally higher in the ANN model. The ANN output has the highest error amplitude value out of 8 samples. Naturally, the average power is not expected to be negative. Except for the 35th sample value of Mdl 2,

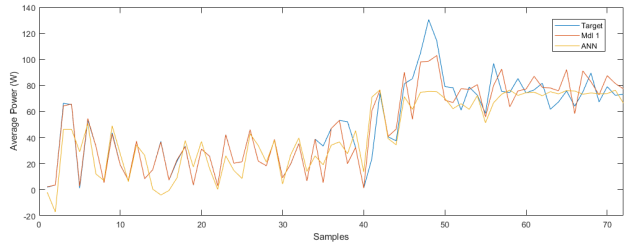

FIGURE 16. Mdl1 vs ANN.

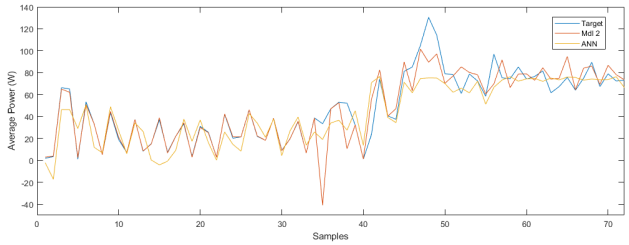

FIGURE 17. Mdl2 vs ANN.

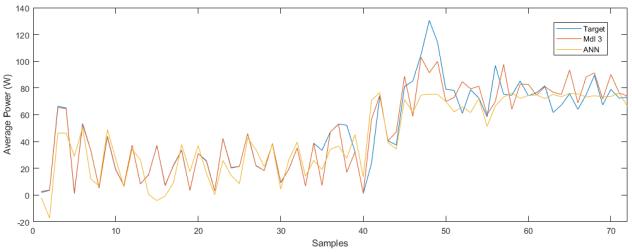

FIGURE 18. Mdl3 vs ANN.

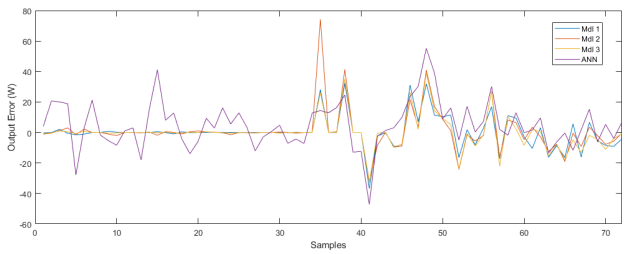

FIGURE 19. Models output errors.

neither Mdl 1 nor Mdl 2 estimated any negative power. On the other hand, the ANN produced negative power, albeit with a small amplitude, in 4 samples. It can be said that the ANFIS models give more successful outputs than the ANN model.

VII. CONCLUSION

In this study, the average power consumed during the welding process in an electrode welding machine was estimated using the characteristics of the emitted sound data. Three ANFIS models created for this purpose yielded very successful results. As the power value increased, the error rate increased and it was possible to obtain smaller errors at lower power values. The biggest advantage of this method is that the energy consumed can also be calculated by using the average power values. Once a sufficient data set is created, the average power consumed can be estimated with high accuracy using a microphone without the need for additional current and voltage measurements.

This study shows that the power or energy consumption of noise-emitting devices, such as welding machines, can be calculated by using sound data. The main limitation of this method is that environmental noise affects the sensing of welding process noise. With active noise cancellation, this can be reduced as much as possible. Another disadvantage is the requirement for a separate Adaptive Neuro-Fuzzy Inference System (ANFIS) model for each welding machine type.

For future studies, average power or energy estimation can be improved by using different feature extraction and estimation methods.

ACKNOWLEDGMENT

The authors would like to thank the administration and faculty of the Kirklareli Vocational High School for their assistance and support in obtaining data for the experimental study and providing access to the necessary equipment.

REFERENCES

[1] X. Yanggui, Z. Shida, G. Shiyi, X. Wanghui, and L. Su, "Research of intelligent welding control system of swing arc narrow gap," in *Proc. IEEE Asia–Pacific Conf. Image Process., Electron. Comput. (IPEC)*, Apr. 2021, pp. 773–775, doi: 10.1109/ipec51340.2021.9421235.

[2] M. Ramakrishnan and V. Muthupandi, "Application of submerged arc welding technology with cold wire addition for drum shell long seam butt welds of pressure vessel components," *Int. J. Adv. Manuf. Technol.*, vol. 65, nos. 5–8, pp. 945–956, Jun. 2012, doi: 10.1007/s00170-012-4230-0.

[3] F. L. Lu, J. F. Wang, C. J. Fan, and S. B. Chen, "A model-free adaptive control of welding pool dynamics during arc welding," in *Proc. IEEE Conf. Cybern. Intell. Syst.*, Chengdu, China, Sep. 2008, pp. 591–595, doi: 10.1109/ICCIS.2008.4670923.

[4] J. Gao, Y. Hong, B. Hong, X. Li, A. Jia, and Y. Qu, "A method of feature extraction of position detection and weld gap for GMAW seam tracking system of fillet weld with variable gaps," *IEEE Sensors J.*, vol. 21, no. 20, pp. 23537–23550, Oct. 2021, doi: 10.1109/JSEN.2021.3106696.

[5] W. Hou, Y. Wei, J. Guo, Y. Jin, and C. Zhu, "Automatic detection of welding defects using deep neural network," *J. Phys., Conf.*, vol. 933, Jan. 2018, Art. no. 012006.

[6] Z. Wang and Y. Xu, "Vision-based seam tracking in robotic welding: A review of recent research," in *Transactions on Intelligent Welding Manufacturing*, vol. 3. Singapore: Springer, 2020, pp. 61–86.

[7] L. Qiang, C. Chao, and S. Chen, "Multi-information sensing and monitoring experimental system of intelligentized welding manufacturing process," in *Transactions on Intelligent Welding Manufacturing*. Singapore: Springer, 2022, pp. 45–75. [Online]. Available: https://link.springer.com/chapter/10.1007/978-981-19-6149-6_3, doi: 10.1007/978-981-19-6149-6_3.

[8] J. Xu, J. Chen, Y. Duan, C. Yu, J. Chen, and H. Lu, "Comparison of residual stress induced by TIG and LBW in girth weld of AISI 304 stainless steel pipes," *J. Mater. Process. Technol.*, vol. 248, pp. 178–184, Oct. 2017, doi: 10.1016/j.jmatprotec.2017.05.014.

[9] B. Hong, A. Jia, Y. Hong, X. Li, J. Gao, and Y. Qu, "Online extraction of pose information of 3D zigzag-line welding seams for welding seam tracking," *Sensors*, vol. 21, no. 2, p. 375, Jan. 2021, doi: 10.3390/s21020375.

[10] S. V. Anand, S. Rastogi, and A. Bhattacharya, "Crack identification and trajectory planning for automatic gas metal arc welding," *Appl. Mech. Mater.*, vol. 911, pp. 89–102, Jan. 2023, doi: 10.4028/p-m8snf9.

[11] R. Brezovnik, J. Cernelic, M. Petrun, D. Dolinar, and J. Ritonja, "Impact of the switching frequency on the welding current of a spot-welding system," *IEEE Trans. Ind. Electron.*, vol. 64, no. 12, pp. 9291–9301, Dec. 2017, doi: 10.1109/TIE.2017.2711549.

[12] S.-H. Song, C.-S. Lee, T.-H. Lim, A. Amanov, and I.-S. Cho, "Fatigue life improvement of weld beads with overlap defects using ultrasonic peening," *Materials*, vol. 16, no. 1, p. 463, Jan. 2023, doi: 10.3390/ma16010463.

[13] S. Chen, D. Yang, J. Liu, Q. Tian, and F. Zhou, "Automatic weld type classification, tacked spot recognition and weld ROI determination for robotic welding based on modified YOLOv5," *Robot. Comput.-Integr. Manuf.*, vol. 81, Jun. 2023, Art. no. 102490, doi: 10.1016/j.rcim.2022.102490.

[14] D. Zhao, Y. Bezgans, N. Vdonin, L. Radionova, L. Glebov, and V. Bykov, "Metallurgical and mechanical attributes of gas metal arc welded high-strength low-alloy steel," *Int. J. Adv. Manuf. Technol.*, vol. 125, nos. 3–4, pp. 1305–1323, Mar. 2023, doi: 10.1007/s00170-023-10807-5.

[15] J. Le, G. Yuan, J. Chen, Z. He, H. Zhang, and X. Chen, "An automatic identification method of welding current and voltage based on visual sensing technology," in *Proc. IEEE 17th Conf. Ind. Electron. Appl. (ICIEA)*, Dec. 2022, pp. 1372–1375, doi: 10.1109/ICIEA54703.2022.10005890.

[16] L. Subashini and M. Vasudevan, "Adaptive neuro-fuzzy inference system (ANFIS)-based models for predicting the weld bead width and depth of penetration from the infrared thermal image of the weld pool," *Metall. Mater. Trans. B*, vol. 43, no. 1, pp. 145–154, Sep. 2011, doi: 10.1007/s11663-011-9570-x.

[17] M. N. Khalid, V. Naranje, and V. H. Gaidhane, "Prediction of best weld quality using artificial neural network," in *Proc. Amity Int. Conf. Artif. Intell. (AICAI)*, Dubai, United Arab Emirates, Feb. 2019, pp. 213–217, doi: 10.1109/AICAI.2019.8701351.

[18] R. M. Nazarov, Z. M. Gizatullin, and E. S. Konstantinov, "Classification of defects in welds using a convolution neural network," in *Proc. IEEE Conf. Russian Young Researchers Electr. Electron. Eng. (ElConRus)*, Jan. 2021, pp. 1641–1644, doi: 10.1109/ElConRus51938.2021.9396301.

[19] M. O. Okwu and O. Adetunji, "A comparative study of artificial neural network (ANN) and adaptive neuro-fuzzy inference system (ANFIS) models in distribution system with nondeterministic inputs," *Int. J. Eng. Bus. Manag.*, vol. 10, Jan. 2018, Art. no. 184797901876842, doi: 10.1177/1847979018768421.

[20] R. S. S. Prasanth and K. H. Raj, "Determination of optimal process parameters of friction stir welding to join dissimilar aluminum alloys using artificial bee colony algorithm," *Trans. Indian Inst. Met.*, vol. 71, no. 2, pp. 453–462, Aug. 2017, doi: 10.1007/s12666-017-1176-9.

[21] Y. Chen, B. Chen, Y. Yao, C. Tan, and J. Feng, "A spectroscopic method based on support vector machine and artificial neural network for fiber laser welding defects detection and classification," *NDT E Int.*, vol. 108, Dec. 2019, Art. no. 102176, doi: 10.1016/j.ndteint.2019.102176.

[22] R. V. Patil, Y. P. Reddy, and A. M. Thote, "Multi-class weld defect detection and classification by support vector machine and artificial neural network," in *Modeling, Simulation and Optimization*. Singapore: Springer, 2021, pp. 429–438. [Online]. Available: https://link.springer.com/chapter/10.1007/978-981-15-9829-6_33#citeas., doi: 10.1007/978-981-15-9829-6_33.

[23] B. Liu, W. Jin, A. Lu, K. Liu, C. Wang, and G. Mi, "Optimal design for dual laser beam butt welding process parameter using artificial neural networks and genetic algorithm for SUS316L austenitic stainless steel," *Opt. Laser Technol.*, vol. 125, May 2020, Art. no. 106027, doi: 10.1016/j.optlastec.2019.106027.

[24] J. Devarai, A. Ziout, and J. A. Qudeiri, "Real-time distortion prediction and optimization of weld sequence using artificial neural network," in *Proc. 14th Int. Conf. Comput. Res. Develop. (ICCRD)*, Shenzhen, China, Jan. 2022, pp. 79–82, doi: 10.1109/ICCRD54409.2022.9730142.

[25] N. Bhandari, S. Khare, R. Walambe, and K. Kotecha, "Comparison of machine learning and deep learning techniques in promoter prediction across diverse species," *PeerJ Comput. Sci.*, vol. 7, p. e365, Feb. 2021.

[26] M. Bayir, E. Yucel, T. Kaya, and N. Yildirim, "Spot welding parameter tuning for weld defect prevention in automotive production lines: An ML-based approach," *Information*, vol. 14, no. 1, p. 50, Jan. 2023, doi: 10.3390/info14010050.

[27] A. Raj, U. Chadha, A. Chadha, R. R. Mahadevan, B. R. Sai, D. Chaudhary, S. K. Selvaraj, R. Lokeshkumar, S. Das, B. Karthikeyan, R. Nagalakshmi, V. Chandramohan, and H. Hadidi, "Weld quality monitoring via machine learning-enabled approaches," *Int. J. Interact. Des. Manuf. (IJIDeM)*, pp. 1–43, Jan. 2023. [Online]. Available: https://link.springer.com/article/10.1007/s12008-022-01165-9, doi: 10.1007/s12008-022-01165-9.

[28] D. Wu, H. Chen, Y. Huang, Y. He, and S. Chen, "Weld penetration identification for VPPAW based on keyhole features and extreme learning machine," in *Proc. IEEE Workshop Adv. Robot. Social Impacts (ARSO)*, Shanghai, China, Feb. 2016, pp. 96–99, doi: 10.1109/ARSO.2016.7736263.

[29] Y. C. Kan and H. Kalkan, "Automatic detection and classification of laser welding defects," in *Proc. Innov. Intell. Syst. Appl. Conf. (ASYU)*, Elazig, Turkey, Oct. 2021, pp. 1–5, doi: 10.1109/ASYU52992.2021.9599064.

[30] P. Jirapipattanaporn and W. Lawanont, "Development of anomaly detection model for welding classification using arc sound," in *Proc. 14th Int. Conf. Knowl. Smart Technol. (KST)*, Jan. 2022, pp. 57–62, doi: 10.1109/kst53302.2022.9729058.

[31] J. Devaraj, A. Ziout, J. A. Qudeiri, R. Baalfaqih, N. Baalfaqh, K. Alahbabi, M. Alnaqbi, and N. Alhosan, "Using machine learning models to predict weld sequence giving minimum distortion," in *Proc. Adv. Sci. Eng. Technol. Int. Conf. (ASET)*, Feb. 2022, pp. 1–6, doi: 10.1109/aset53988.2022.9734845.

[32] J. Guo, Y. Liu, and G. Wu, "Construction of welding quality intelligent judgment system," in *Proc. IEEE Int. Conf. Mechatronics Autom. (ICMA)*, Tianjin, China, Aug. 2019, pp. 141–145, doi: 10.1109/ICMA.2019.8816409.

[33] I. Kiyak, G. Gökmen, and G. Koçyigit, "Lifetime prediction for a cell-on-board (COB) light source based on the adaptive neuro-fuzzy inference system (ANFIS)," *J. Nanomaterials*, vol. 2021, pp. 1–10, Mar. 2021, doi: 10.1155/2021/6681335.

[34] M. Sahin and R. Erol, "Prediction of attendance demand in European football games: Comparison of ANFIS, fuzzy logic, and ANN," *Comput. Intell. Neurosci.*, vol. 2018, pp. 1–14, Aug. 2018, doi: 10.1155/2018/5714872.

[35] M. Guzel, I. Kok, D. Akay, and S. Ozdemir, "ANFIS and deep learning based missing sensor data prediction in IoT," *Concurrency Comput., Pract. Exper.*, vol. 32, no. 2, p. e5400, Jan. 2020, doi: 10.1002/cpe.5400.

[36] J.-S. R. Jang, "ANFIS: Adaptive-network-based fuzzy inference system," *IEEE Trans. Syst., Man, Cybern.*, vol. 23, no. 3, pp. 665–685, May/Jun. 1993, doi: 10.1109/21.256541.

[37] M. Yucel, F. V. Celebi, M. Torun, and H. H. Goktas, "Adaptive neuro-fuzzy based gain controller for erbium-doped fiber amplifiers," *Adv. Electr. Comput. Eng.*, vol. 17, no. 1, pp. 15–20, 2017, doi: 10.4316/aece.2017.01003.

[38] T. C. Akinci, O. Akgun, T. C. Akinci, and S. Seker, "Fast Fourier transformation of welding machines and their classification with acoustic method," *Mechanics*, vol. 23, no. 4, pp. 588–593, Sep. 2017, doi: 10.5755/j01.mech.23.4.14876.

[39] L. Gunaydin, T. C. Akinci, G. G. K. Gokmen, and O. Akgun, "Analysis of sounds generated from welding machine while in idle and operational mode by acoustic method," *Appl. Researches Technics, Technol. Educ.*, vol. 3, no. 3, pp. 214–223, 2015, doi: 10.15547/artte.2015.03.002.

[40] R. Neitzel and N. Seixas, "The effectiveness of hearing protection among construction workers," *J. Occupational Environ. Hygiene*, vol. 2, no. 4, pp. 227–238, Apr. 2005, doi: 10.1080/15459620590932154.

[41] T. F. W. Embleton, "Technical assessment of upper limits on noise in the workplace," *Noise News Int.*, vol. 5, no. 4, pp. 203–216, Dec. 1997, doi: 10.3397/1.3703031.

[42] R. S. Herrera, P. SalmerÓn, and H. Kim, "Instantaneous reactive power theory applied to active power filter compensation: Different approaches, assessment, and experimental results," *IEEE Trans. Ind. Electron.*, vol. 55, no. 1, pp. 184–196, Jan. 2008, doi: 10.1109/TIE.2007.905959.

[43] H. Hafezi, "Instantaneous reactive power control and its model for single phase loads," Ms.C. thesis, Dept. Electr. Electron. Eng., Graduate School Natural Appl. Sci., Dokuz Eylul Univ., Izmir, Turkey, 2013, pp. 22–35.

[44] S. Karasu and Z. Saraç, "Classification of power quality disturbances with Hilbert–Huang transform, genetic algorithm and artificial intelligence/machine learning methods," *J. Polytech.-Politeknik Dergisi*, vol. 23, no. 4, pp. 1219–1229, 2020, doi: 10.2339/politeknik.508773.

GOKHAN GOKMEN received the B.S., M.S., and Ph.D. degrees in electric education in Istanbul, Turkey, in 1996, 2000, and 2006, respectively. He was a Research Assistant and an Assistant Professor with the Faculty of Technical Education, Marmara University, Istanbul, from 1998 to 2009 and from 2009 to 2015, respectively. He was an Associate Professor with the Department of Mechatronics Engineering, Marmara University, from 2015 to 2018, where he has been a Full Professor, since 2018. His research interests include artificial neural networks, deep learning, machine learning, measurement, signal processing, and data analysis.

TAHIR CETIN AKINCI (Senior Member, IEEE) received the B.S. degree in electrical engineering, and the M.S. and Ph.D. degrees, in 2005 and 2010, respectively. He was a Research Assistant with Marmara University, Istanbul, Turkey, from 2003 to 2010, and an Associate Professor with Istanbul Technical University (ITU), from 2016 to 2021, where he has been a Full Professor with the Department of Electrical Engineering, since 2021. He has been a Visiting Scholar with the University of California at Riverside (UCR), since 2021. His research interests include artificial neural networks, deep learning, machine learning, cognitive systems, signal processing, and data analysis.

GOKHAN KOCYIGIT received the B.S., M.S., and Ph.D. degrees in electric education in Istanbul, Turkey, in 1996, 1999, and 2008, respectively. He was a Research Assistant with the Faculty of Technical Education, Marmara University, Istanbul, from 1997 to 2011. He has been an Assistant Professor with the Department of Electrical and Electronics Engineering, Trakya University, Edirne, Turkey, since 2011. His research interests include high voltage, electric power transmission, electrical circuits, digital video, and computer graphics.

ISMAIL KIYAK received the B.S., M.S., and Ph.D. degrees in electric education in Istanbul, Turkey, in 2000, 2005, and 2010, respectively. He was a Research Assistant with the Faculty of Technical Education, Marmara University, Istanbul, from 2001 to 2012. He was an Assistant Professor and an Associate Professor with the Department of Electric and Electronics Engineering, Marmara University, from 2013 to 2016 and from 2016 to 2021, respectively, where he has been a Full Professor, since 2021. His research interests include artificial intelligence-based lighting control, semiconductor lighting, smart city lighting, measurement, special lighting systems, and renewable energy-based lighting systems.

M. ILHAN AKBAS (Member, IEEE) received the B.S. and M.S. degrees from the Department of Electrical and Electronics Engineering, Middle East Technical University, and the Ph.D. degree in computer engineering from the University of Central Florida. He is currently an Assistant Professor with the Department of Electrical Engineering and Computer Science, Embry-Riddle Aeronautical University. He has industry experience in projects with multinational defense industry partners and large enterprises. His research interests include autonomous cyber-physical systems, validation and verification, wireless networks, and mobile computing. He is a member of ACM, AAAI, and SAE.